

Spatial genetic subdivision among populations of *Pampus chinensis* between China and Pakistan: testing the barrier effect of the Malay Peninsula

Yuan Li¹, Tianxiang Gao^{2,3,*}, Yongdong Zhou³ and Longshan Lin^{1,*}

¹ Third Institute of Oceanography, Ministry of Natural Resources, Xiamen 361005, PR China

² National Engineering Research Center for Marine Aquaculture, Zhejiang Ocean University, Zhoushan 316022, PR China

³ Key Laboratory for Technology Research on Sustainable Utilization of Marine Fishery Resources, Zhoushan 316021, PR China

Received 12 October 2018 / Accepted 13 February 2019

Handling Editor: Ziniu Yu

Abstract – Tissue samples from 84 *Pampus chinensis* individuals were collected from four geographic regions within the Indo–Pacific Ocean and analyzed using mitochondrial and nuclear DNA markers. Distinct genetic heterogeneity was found for both types of markers between Chinese and Pakistani populations, while the diversity of this species was high in all populations. In combination with published information on marine species with similar distributions, these results suggested that the Malay Peninsula, or a less effective supplement, played a role in shaping the contemporary genetic structure. This population structure was presumably reflected in *P. chinensis*, whose populations were genetically isolated during Pleistocene glaciations and then did not experience secondary contact between previous refuge populations. However, *P. chinensis* showed genetic continuity in China or Pakistan, which indicated that the populations in different geographical regions constituted a single panmictic stock with high gene flow, respectively. The spatial genetic subdivision evident among populations indicates that *P. chinensis* in this Indo–Pacific region should be managed as different independent stocks to guide the sustainability of this fisheries resource.

Keywords: Phylogeography / genetic structure / mitochondrial DNA / microsatellite / isolation by distance

1 Introduction

Insight into the genetic population structure of marine economic fishes facilitates the identification of appropriate management units (e.g., stock rather than management agency boundaries) (Barnes et al., 2015). Intraspecific gene flow relies on the connectivity between different areas, and physical barriers to such connectivity can lead to spatial genetic subdivision (Barnes et al., 2015; Divya et al., 2018). These barriers can form discrete population units, in which genetic drift has a much greater influence on population dynamics than gene flow, and these units are described as phylogeographic populations or patterns (Koizumi et al., 2006; Ovenden, 2013). The influence of barriers may be a factor in the population dynamics of fishes, but their influence is not easily assessed or considered in isolation by distance, which is the model that is commonly used to explain population structures in widely

distributed fish species (Sun et al., 2017). Therefore, to better understand the mechanisms of population structuring, the influence of physical and biological factors need to be assessed (Barnes et al., 2015).

In some cases, some species populations became genetically isolated during the last glacial maximum (LGM); subsequent restructuring presumably reflects a period of secondary contact (Liu et al., 2012). During the LGM, the sea level dropped drastically below the present level of marginal seas, which caused extensive habitat loss and population fragmentation for many marine species due to the emergence of new dispersal barriers (Wang and Sun, 1994). With the rise of sea levels after the LGM, the surviving marine fish would have quickly recolonized from the refugia and reoccupied the newly available habitats in a process coupled with restructuring based on secondary contact between refuge populations (Avice, 2009).

Pampus chinensis (Euphrasen, 1788) has economic value and is widely distributed in the Indo–West Pacific Oceans (Liu et al., 2002; Yamada et al., 2009). As with most Stromateidae fishes, the species can be distinguished by a

*Corresponding authors: gaotianxiang0611@163.com;
linlsh@tio.org.cn

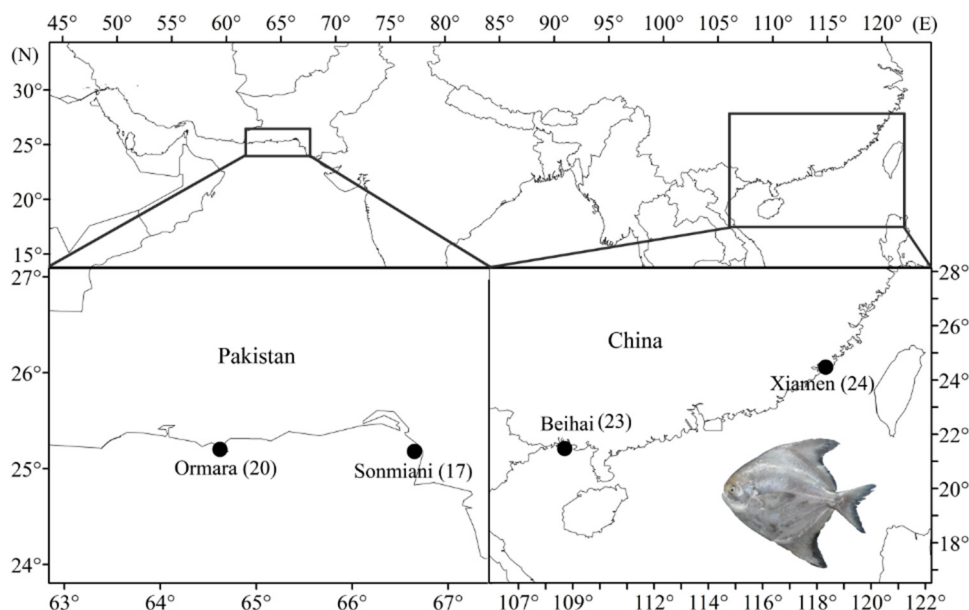


Fig. 1. Locations of populations used in this study.

diamond body shape that obviously differs from other congeneric species (Liu et al., 2002; Yamada et al., 2009). There is an ongoing debate about the strength of the relationship in marine species between the pelagic larval duration and the degree of genetic connectivity (Selkoe and Toonen, 2011). The dispersal capability, wide distribution, and habitat type make *P. chinensis* a good model organism for testing the complex effects of sea level change during the Pleistocene and of current intricate hydrological conditions on fauna living in the coastal areas of China and Pakistan. With its high nutritional value and good taste, this species has declined rapidly in the past few decades due to overfishing and commercial pressure (Pillai and Menon, 2000; Zheng et al., 2003; Siyal, 2013). As little is known about the genetic diversity and structure of this species, the present study had two objectives. First, we conducted a genetic survey of the species and investigated the level and distribution of genetic diversity among populations using both mitochondrial (mt) DNA and microsatellite DNA markers. Second, we tested for the existence of genetic structures within and among populations of *P. chinensis* to determine whether the Malay Peninsula works as a major potential geographical barrier in the sampling range.

Knowledge regarding the population structure and level of variation in this species will provide valuable insights into proper conservation strategies to preserve this resource and to address genetic resource problems that these populations face. Moreover, these findings help to reveal the evolutionary mechanisms that shape the phylogeography of marine fauna living in coastal areas.

2 Materials and methods

2.1 Sample collection

A total of 84 individuals of *P. chinensis* were sampled in 2011–2014 from four locations in the Indian and Pacific Oceans: two locations in China (Xiamen and Beihai) and two

locations in Pakistan (Ormara and Sonmiani) (Fig. 1). After specimen identification, back muscle tissues were excised and preserved in 95% ethanol for DNA extraction and subsequent molecular experiments.

2.2 DNA extraction and amplification

Genomic DNA was isolated from muscle tissue using proteinase *K* digestion and extracted using standard phenol–chloroform extraction (Sambrook et al., 1989). Extracted DNA was checked using 1.5% agarose gel electrophoresis and then stored at -20°C for PCR amplification.

2.2.1 Control region amplification

The mtDNA control region (CR) was amplified with the primers F-gao, 5'-GAAGTTAAAATCTTCCCTTTTGC-3' (forward), and R-gao, 5'-GGCCCTGAAGTAGGAACCAAA-3' (reverse), which is a 438–439 bp fragment. Each PCR experiment was performed in a 25 μL reaction mixture containing 17.5 μL of ultrapure water, 2.5 μL of $10 \times$ PCR buffer, 2 μL of dNTPs, 1 μL of each primer (5 μM), 0.15 μL of Taq DNA polymerase, and 1 μL of DNA template. PCR amplification was performed under the following conditions: 5 min of initial denaturation at 95°C ; 30 cycles of 45 s at 94°C for denaturation, 45 s at 50°C for annealing, and 45 s at 72°C for extension; and a final extension at 72°C for 10 min. Successful amplifications were purified and both strands were sequenced using the same primers as for conduct PCR. The newly isolated nucleotide sequences were assigned GenBank accession numbers KY113351–KY113376. Two additional CR sequences from *Pampus argenteus* were used as the out-group.

2.2.2 Microsatellite amplification

Seven microsatellite loci were amplified with primers developed by Yang et al. (2006) (Tab. 5). The samples were amplified using a 25 μL PCR mixture containing 17.25 μL of

ultrapure water, 2.5 μL of $10 \times$ PCR buffer (including MgCl_2), 2 μL of dNTPs, 1 μL of fluorescently labeled M13R forward primer, 1 μL of reverse primer, 0.25 μL of Taq polymerase, and 1 μL of genomic DNA (10 ng). All loci were initially screened using the following PCR protocol: 5 min at 94 °C followed by 35 cycles of 45 s at 94 °C, 45 s at 50–58 °C, 45 s at 72 °C, and a final step for 15 min at 72 °C. The reactions were then exposed to 72 °C for 45 min and held at 4 °C until required for further analysis. Amplicons were diluted 20-fold with ultrapure Milli-Q water before being further diluted (1:5) in formamide containing the LIZ-500 size standard. The samples were then separated by capillary gel-electrophoresis following the manufacturer's instructions. To score the consistency of the microsatellite fragments, nearly 20% of samples were stored as replicates (Williams et al., 2015).

2.3 mtDNA sequence data analysis

Mitochondrial DNA sequences were edited and aligned using DNASTAR. Polymorphic sites, number of haplotypes, and molecular diversity indices for each population were calculated in Arlequin 3.5 (Excoffier and Schneider, 2005).

Genetic relationships among haplotypes were reconstructed using the neighbor-joining (NJ) method implemented with 1000 bootstrap replicates in MEGA 5.0 under the chosen substitution model HKY (Tamura et al., 2011). To evaluate the genetic differentiation between sampling populations, pairwise genetic divergences (F_{ST}) were estimated in Arlequin. Analysis of molecular variation (AMOVA) was performed in Arlequin to investigate the partitioning of genetic variation within and among populations, along with hierarchical analysis by population groupings to investigate the possible effects of the major potential geographical barrier (the Malay Peninsula) on the phylogeographic pattern.

Historical demography/spatial expansions were inferred by a neutrality test and mismatch distribution analysis implemented in Arlequin. Deviations from neutrality were tested with Fu's F_S and Tajima's D . Nucleotide mismatch distributions were used to test for population growth and spatial range expansions. A molecular clock-based time estimate provided an approximate timeframe for evaluating phylogeographical hypotheses. Finally, Bayesian skyline plots (BSPs) were created with BEAST 1.7 (Drummond et al., 2012). In the present study, a sequence divergence rate of 5–10%/Myr (Bermingham et al., 1997; Bowen et al., 2001) was applied to the control region sequences of *P. chinensis* under the HKY model in BEAST (Bowen et al., 2001; Sukumaran et al., 2017). BSPs revealed a detailed demographic history of population size changes, from which we could determine whether the populations of this species had undergone population expansion in the late Pleistocene.

2.4 Microsatellite DNA data analysis

Microsatellite alleles were called using Geneious ver. 7 against an internal size standard. To examine the genetic diversity of *P. chinensis*, the number of alleles (N_A), observed heterozygosity (H_O) and expected heterozygosity (H_E) were estimated using POPGENE 1.32 (Yeh et al., 2000).

Polymorphism information content (PIC) was calculated using MS tools.

Deviations from the Hardy–Weinberg equilibrium (HWE) and linkage disequilibrium of each locus within each site were checked by GENEPOP 3.4 (Raymond and Rousset, 1995). The presence of null alleles and potential scoring errors were addressed using MicroChecker 2.2.3 (van Oosterhout et al., 2004). FSTAT 2.9.3 (Goudet, 2001) was used to calculate the value of allelic richness (R_S) and assess the values of Φ_{ST} .

Bayesian cluster analysis of the microsatellite data was performed using STRUCTURE (Pritchard et al., 2000). Population groups were simulated from $K=1-9$, with each K being run 10 independent times; possible mixed ancestry and correlated allele frequencies were assumed, and 1,000,000 Markov chain Monte Carlo (MCMC) steps, discarding the first 100,000 steps, were used. To estimate the most likely number of clusters (K), an ad hoc approach (Pritchard et al., 2000) was taken by obtaining the mean posterior probability of the data [$L(K)$]; the data set was analyzed for $K=2$, where the value did not increase and either peaked or plateaued as expected.

Bottleneck 1.2.02 (Piry et al., 1999) was used to detect the evidence of recent bottleneck events under three different mutation models: the infinite allele model (IAM), the stepwise mutation model (SMM), and the two-phase mutation model (TPM). In each model, 95% single-step mutations and 5% multiple steps mutations with 1000 simulation iterations were set, as recommended (Zeng et al., 2012). We also proposed a graphical descriptor of the shape of the allele frequency distribution (mode shift indicator), which could differentiate between bottlenecked and stable populations (Luikart and Cornuet, 1998).

3 Results

In general, the methods using mtDNA and microsatellite data to analyze genetic diversity were very similar. The different marker types in this study were in accordance and therefore provided further insights into the evolutionary history of *P. chinensis*.

3.1 Mitochondrial DNA variation

After a conserved 70 bp portion at 5' end of the tRNA^{pro} gene was deleted, a 368–369 bp segment of the CR was obtained from 84 specimens. These sequences were polymorphic at 30 nucleotide sites, which comprised 26 transitions, 6 transversions, and 1 indel/deletion. The overall A+T ratio was 68%, representing an AT bias. The haplotype diversity (h) ranged from 0.7789 (Ormara) to 0.8804 (Xiamen) (total 0.9174), and the nucleotide diversity (π) ranged from 0.0078 (Sonmiani) to 0.0128 (Xiamen) (total 0.0238) (Tab. 1). The nucleotide diversities in Chinese samples were higher than those in the Pakistani samples (Tab. 1).

All sequences defined 26 haplotypes among 84 specimens, and no haplotype was found more than three times (Fig. 2). The Chinese and Pakistani populations shared no haplotypes, though four haplotypes were shared between the populations of Xiamen and Beihai; the same result was found in the Pakistani populations, which also shared four shared

Table 1. Summary statistics for mtDNA molecular indices of *P. chinensis*.

Populations	Number	Date	NH	NUH	$h \pm SD$	$\pi \pm SD$	$k \pm SD$
Sonmiani	17	2011.10	9	5	0.8309 ± 0.0846	0.0078 ± 0.0048	2.8824 ± 1.5930
Ormara	20	2012.12	8	4	0.7789 ± 0.0678	0.0084 ± 0.0051	3.1000 ± 1.6797
Beihai	23	2012.08	7	3	0.8261 ± 0.0524	0.0103 ± 0.0060	3.7866 ± 1.9792
Xiamen	24	2014.04	8	6	0.8804 ± 0.0387	0.0128 ± 0.0072	4.7174 ± 2.3921
Total	84	—	26	—	0.9174 ± 0.0143	0.0238 ± 0.0123	8.7731 ± 4.0882

Note: NH, numbers of haplotypes; NUH, numbers of unique haplotype; h , haplotype diversity; π , nucleotide diversity; k , average number of pairwise differences.

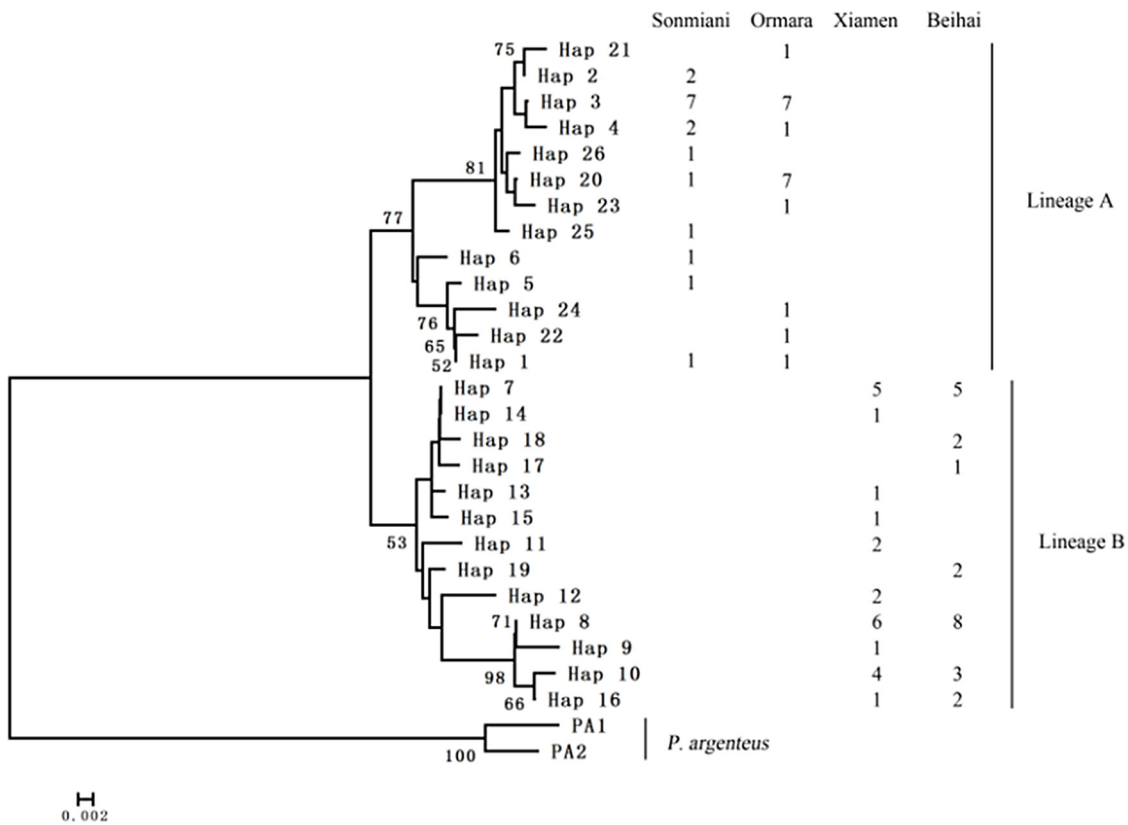


Fig. 2. Neighbor-joining tree and distribution of the control region haplotypes of *P. chinensis*. *P. argenteus* was used as the out-group. Bootstrap supports of >50 in 1000 replicates are shown.

haplotypes. Unique haplotypes were also found in each population: six were found in Xiamen, three in Beihai, five in Sonmiani, and four in Ormara (Tab. 1 and Fig. 2).

These phylogenetic analyses revealed two deeply divergent lineages that were geographically concordant (Fig. 2). All haplotypes fell into two deeply separated lineages, suggesting that at least two differentiated populations had been successfully recruited. Lineage A exclusively comprised the Pakistani populations, and Lineage B occurred in China. A total of 44% (37/84) of the samples were derived from Lineage A, whereas 56% (47/84) were derived from Lineage B.

The F_{ST} values between samples from China and Pakistan varied from 0.714 to 0.755 and were statistically significant. However, the F_{ST} values between the Chinese samples or

between the Pakistani samples were very low and nonsignificant (Tab. 2). The AMOVA of haplotype variability among samples yielded an $F_{ST}=0.644$ ($P < 0.001$) as one gene pool, and divergence was much larger and was attributable to 66.72% genetic variation among populations (Tab. 3). To further investigate the possible effects of major potential geographical barriers (Malay Peninsula), the populations of Xiamen and Beihai were treated as a group and those of Ormara and Sonmiani constituted another group, which yielded significant statistical differences between the two groups ($F_{CT}=0.739$, $P < 0.001$) (Tab. 3). The Mantel test showed significant genetic variation that could be explained by geographic distance, with a reasonable fit of the model ($R^2=0.742$, $P < 0.05$).

Table 2. *P. chinensis* pairwise standardized mitochondrial F_{ST} (below diagonal) and microsatellite Φ_{ST} (above diagonal) values.

Populations	Sonmiani	Ormara	Beihai	Xiamen
Sonmiani		0.008	0.306*	0.344*
Ormara	-0.010		0.306*	0.345*
Beihai	0.755*	0.750*		0.049
Xiamen	0.715*	0.714*	-0.026	

Significant results were accepted at $P < 0.05$ and are denoted by *.

Table 3. Analysis of molecular variance (AMOVA) of *P. chinensis* populations based on mitochondrial control region sequences.

Source of variation	Sum of squares	Percentage	F -statistic	P
<i>One gene pool</i>				
Among populations	215.672	64.39	$F_{ST} = 0.644$	0.000
Within populations	148.411	35.61		
<i>Two gene pools (S, O) (X, B)</i>				
Among groups	213.588	73.86	$F_{CT} = 0.73864$	0.000
Among populations within groups	2.085	-0.56	$F_{SC} = -0.02138$	0.734
Within populations	148.411	26.69	$F_{ST} = 0.73306$	0.349

The shapes of the mismatch distributions were multimodal in all four populations but tended to be unimodal in Lineage A or B (Fig. 3). However, neutrality tests of Fu's F_S yielded significantly negative values. Neither the SSD nor the HRI were statistically significant in Lineage A or B (Tab. 4). These data indicate that none of the distributions deviated from an expansion model and support a fit between the observed and the expected distributions. The τ value of mismatch distributions provided a general population expansion time, and the τ values of Lineages A and B were 1.373 and 7.705, respectively (Tab. 4). Therefore, the time since the expansion of Lineages A and B was estimated to be 37,000–74,000 and 209,000–418,000 years ago, respectively. The BSP results indicated that the effective population size of Lineage A increased sharply after the LGM, approximately 25,000 years before the present, and the effective population size of Lineage B slowly increased from 200,000 years ago during the Quaternary Period (Fig. 4).

3.2 Microsatellite variation

Seven microsatellite loci were employed to estimate the diversity and divergence between the *P. chinensis* populations. The number of alleles per locus (A) ranged from 5 (Par 08/Par 20) to 21 (Par 17) (Tab. 5), and the number of alleles per population ranged from 27 (Sonmiani) to 42 (Xiamen/Beihai). The number of individuals genotyped across each geographical region ranged from 27 to 42, reflecting the availability of samples. The heterozygosities were higher on average among the samples from the Chinese populations ($H_E = 0.559-0.565$)

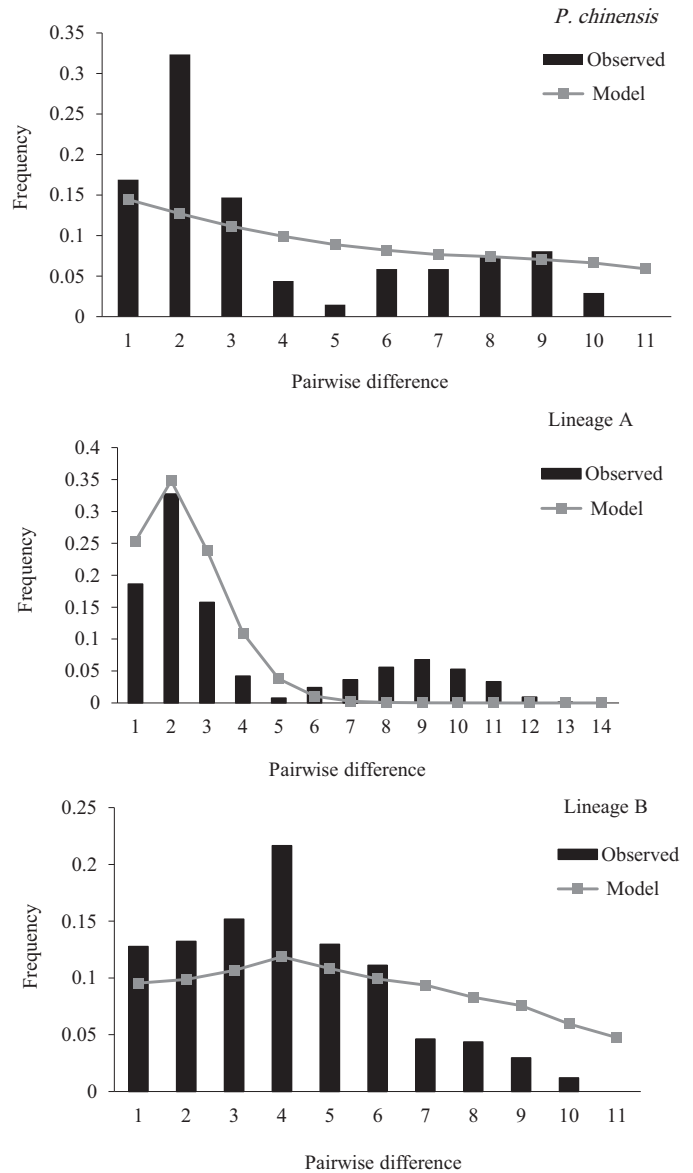


Fig. 3. Mismatch distributions of control region haplotypes of *P. chinensis*.

than from the Pakistani populations ($H_E = 0.429-0.474$). The PIC values were higher on average among the Chinese populations (>0.5) than they were among the Pakistani populations (<0.5) (Tab. 5), suggesting that the Chinese allele set had high diversity.

However, a distinct geographical trend appeared in the levels of overall microsatellite diversity. To test the Micro-Checker results, the two loci were checked for departures from HWE with heterozygote excess, but none remained significant after Bonferroni correction. Likewise, all loci were included for subsequent analyses.

An assessment of Φ_{ST} estimates for spatial population structure indicated high and significant structuring among individuals between Chinese and Pakistani populations (values of 0.306–0.345) (Tab. 2). However, the pairwise Φ_{ST} values between the samples from China or between the

Table 4. Summary of the neutral test and goodness-of-fit test for *P. chinensis*.

Groups	<i>n</i>	<i>N</i>	Tajima's <i>D</i>		Fu's <i>F_s</i>		Goodness-of-fit test				
			<i>D</i>	<i>P</i>	<i>F_s</i>	<i>P</i>	τ	θ_0	θ_1	SSD	HRI
All	84	26	-0.094	0.480	-2.454	0.079	10.555	0.000	7.200	0.058 ns	0.072 ns
Lineage A	37	13	-0.547	0.347	-3.406	0.044	1.373	0.000	99999	0.030 ns	0.065 ns
Lineage B	47	13	-0.468	0.721	-0.987	0.036	7.705	0.002	8.076	0.034 ns	0.066 ns

Note: Number of individuals (*n*), number of haplotypes (*N*), Tajima's *D* and Fu's *F_s*, corresponding *P*-value, and mismatch distribution parameter estimates for each lineage are also indicated. τ (95% CI) is the time of initiation of population expansion; θ_0 and θ_1 are the θ parameters before and after expansion, respectively; SSD and HRI are the sum of squared deviations and raggedness index, respectively. ns, *P* > 0.05.

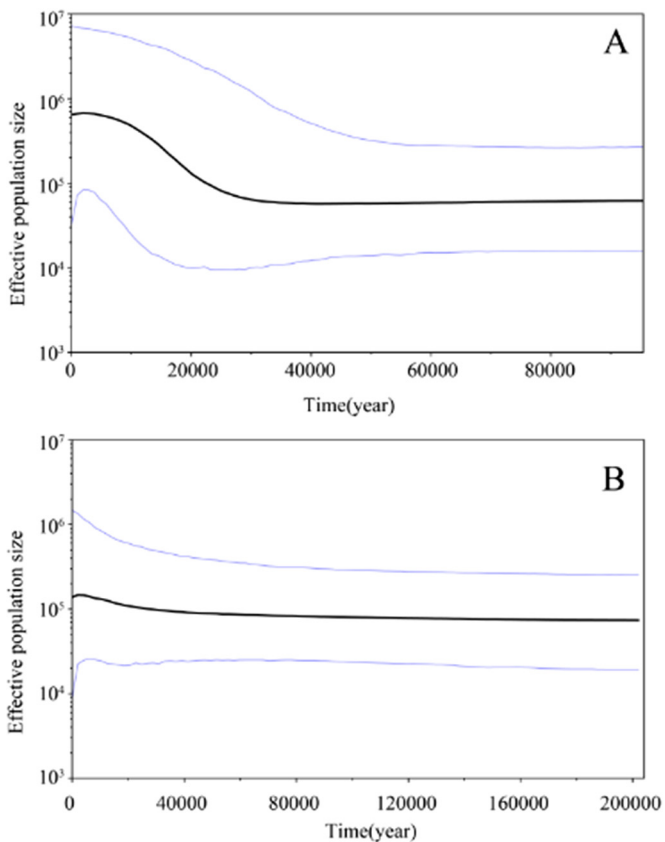


Fig. 4. Bayesian skyline plots showing $N_{ef}T$ (N_{ef} = effective population size; T = generation time) changes over time for *P. chinensis* based on the CR sequences. The upper and lower limits of the blue trend represent the 95% confidence intervals of the highest posterior density (HPD) analysis. The black line is the median estimate for $N_{ef}T$.

samples from Pakistan within the same ocean basin were very low and nonsignificant (Tab. 2). Thus, these populations were pooled together in accordance with the mitochondrial DNA results.

The program STRUCTURE revealed the two most likely genetic clusters when all sample sets were included in the analysis. Notably, the likelihoods estimates for $\Delta K = 2$ did not increase and neither peaked nor plateaued as expected (Latch

et al., 2006). The genetic clusters showed spatial structuring, with one cluster (cluster 1) comprising 98% membership from Sonmiani and Ormara, and the other (cluster 2) comprising the most individuals (98%) from Chinese populations (Fig. 5). In addition, there was concordance between microsatellite clade membership and the genetic partitioning found between the groupings identified by mtDNA (Fig. 2).

The results of the genetic bottleneck analysis were assessed by the Wilcoxon sign-rank test under three models of microsatellite evolution (IAM, TPM, and SMM) (Tab. 6). No significant heterozygosity excess was detected in any population under the three models, implying that no genetic bottlenecks were detected in this species due to mutation-drift equilibrium. The normal L-shaped distribution patterns of the allele frequencies in all populations were found under the mode shift test, which also indicated the absence of bottleneck events. Therefore, no studied population of *P. chinensis* had suffered from a recent genetic bottleneck.

4 Discussion

Mitochondrial and nuclear DNA markers have different mutation rates, enabling the detection of contemporary gene flow and deeper separations between populations. The relatively lower mutation rates of mtDNA allow for the reconstruction of population events reaching back several thousand years, whereas the larger mutation rates of microsatellites yield insight into contemporary levels of gene flow (Liu et al., 2012). Therefore, the results of this study provide insights into the general features of the *P. chinensis* population structure.

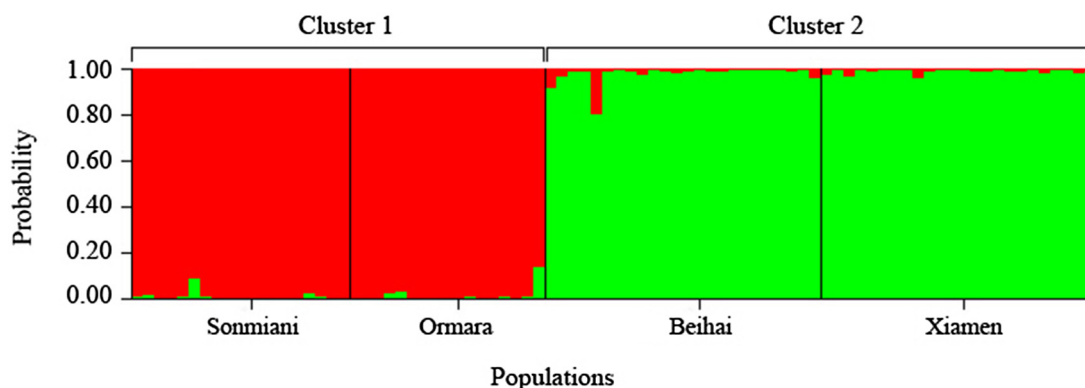
4.1 Genetic diversity

The estimated genetic diversity was high in *P. chinensis* populations according to both the mtDNA and microsatellite analyses. These data suggest that the *P. chinensis* populations were much larger at one time. The reasons for the current high diversity of this species may be related to the following aspects. First, the species is distributed over a wide geographical area and diverse habitats. *P. chinensis* is distributed in the Chinese sea, the Bay of Bengal, the Arabian Sea, and even in coastal Southeastern Asia. The long coastline

Table 5. Summary statistics for the variability of seven polymorphic microsatellite loci in four *P. chinensis* populations.

Populations	Locus								Average
	Index	par03	par08	par20	par05	par12	par18	par17	
Sonmiani	N_A	7	2	1	3	1	3	10	3.86
	R_S	3.400	1.990	1.000	1.740	1.000	1.380	5.160	2.240
	H_O	0.725	0.512	0	0.437	0	0.28	0.828	0.397
	H_E	0.789	0.737	0	0.579	0	0.211	1	0.474
	PIC	0.665	0.374	0.000	0.354	0.000	0.247	0.781	0.346
Ormara	N_A	7	2	1	4	1	4	12	4.43
	R_S	4.620	1.970	1.000	2.050	1.000	1.360	3.550	2.220
	H_O	0.807	0.508	0	0.528	0	0.273	0.74	0.408
	H_E	0.706	0.647	0	0.706	0	0.294	0.647	0.429
	PIC	0.752	0.372	0.000	0.431	0.000	0.253	0.701	0.358
Beihai	N_A	9	3	5	4	1	10	10	6.00
	R_S	4.023	1.600	2.150	2.550	1.000	5.850	4.300	3.070
	H_O	0.522	0.318	0.458	0.458	0.000	0.833	0.762	0.479
	H_E	0.768	0.385	0.548	0.621	0.000	0.847	0.786	0.565
	PIC	0.733	0.344	0.497	0.529	0.000	0.808	0.748	0.523
Xiamen	N_A	8	4	4	4	2	9	11	6.00
	R_S	4.110	2.960	1.350	2.450	1.040	4.990	3.540	2.920
	H_O	0.417	0.750	0.292	0.500	0.042	0.750	0.667	0.488
	H_E	0.773	0.676	0.267	0.604	0.042	0.816	0.733	0.559
	PIC	0.729	0.594	0.248	0.507	0.040	0.777	0.692	0.512

Note: N_A : allelic number, R_S : allelic richness, H_O : observed heterozygosity, H_E : expected heterozygosity, PIC: polymorphism information content.

**Fig. 5.** Results of the STRUCTURE analysis from seven microsatellite loci in *P. chinensis* ($K=2$). Vertical lines are proportional to the probability of individual membership in the simulated cluster.**Table 6.** Results of Wilcoxon's heterozygosity excess test and Mode shift indicator for a genetic bottleneck in the four populations of *P. chinensis*.

Populations	Wilcoxon sign-rank test			Mode shift
	IAM	TPM	SMM	
Sonmiani	0.109	0.922	0.969	L
Ormara	0.688	0.922	0.922	L
Beihai	0.422	0.984	0.992	L
Xiamen	0.711	0.980	0.992	L

created a diverse marine ecological environment, allowing this species to successfully adapt to local habitat conditions. Moreover, the attrition of individuals from populations with subsequent recruitment may have contributed to the levels of variation now seen in different locations (Zheng et al., 2003; Lu et al., 2016). Second, the species has not suffered from a genetic bottleneck event. The Wilcoxon sign-rank test under three models of microsatellite evolution showed that none of the studied populations of *P. chinensis* suffered from a genetic bottleneck in recent history; likewise, less genetic variation has been lost.

Overall, the data set for *P. chinensis* indicated that the populations that encompassed a wide geographical area retained high genetic diversity.

4.2 Population differentiation

The majority of variation in *P. chinensis* was found among, rather than within, populations, and this difference was great and significant. This finding may be a reflection of *P. chinensis* having two population lineages that are genetically indistinguishable. The numbers of unique haplotype/diagnostic alleles were possibly signs of differentiation among the populations following selection or genetic drift from the ancestral genetic environment. On the other hand, these haplotypes/alleles may represent new mutations (such as deletions or insertions) that have appeared among populations following their initial dispersal after speciation events (Lu et al., 2016).

Many authors have suggested that Pleistocene climatic oscillations had profound effects in shaping the present phylogeographical patterns and genetic structures of marine species (Liu et al., 2007, 2012; Williams et al., 2015; Qiu et al., 2016). This study provides clear evidence of genetic differentiation between the populations of *P. chinensis* inhabiting the Pacific Ocean (China) and the Indian Ocean (Pakistan). These results are consistent with the results for many other marine species that were similarly distributed in these waters, e.g., crab (Lavery et al., 1996), prawn (Benzie et al., 2002), lobster (Yellapu et al., 2016), shark (Giles et al., 2014), and damselfish (Raynal et al., 2014), which all showed strong and significant population structures, despite their great potential for long-distance larval dispersal. The clearest indication of this differentiation was the existence of fixed haplotype differences and distinct lineages in the two oceans (Lavery et al., 1996). The two lineages of *P. chinensis* found from the combined genetic data set corresponded to geographic locations, reflecting the presence of distinct populations in the past that were not likely admixed (Williams et al., 2015).

Moreover, both the pairwise population differences and the genetic distance were directly proportional to geographic distance among all the populations, and a pattern of isolation by distance was observed, suggesting that *P. chinensis* populations have acquired significantly different genetic structures between the Pacific and Indian Oceans (Figs. 2 and 5). Two hypotheses explain this result in this species. First, the Malay Peninsula acted as a geographic barrier that divided *P. chinensis* into differentiated populations without mixed exchange, thereby blocking gene flow between the Pacific and Indian Oceans. Though this explanation is plausible, another explanation is equally likely. Assuming that an individual in each generation could effectively migrate into another reproductive population, tiny gene exchanges could prevent genetic differentiation caused by genetic drift or natural selection (Slatkin, 1987). Obviously, the genetic results showed that either there was no gene exchange between the Pacific and Indian Oceans or, if some individuals had an opportunity to exchange genes through the Malacca Strait, the effective supplement to the new stock was almost nonexistent or very weak. Similarly, the dichotomous genetic

differentiation into the Pacific and Indian lineages has also been reported in other marine species, such as coastal fauna and mangrove species (Lavery et al., 1996; Chenoweth et al., 1998; Williams and Benzie, 1998; Benzie, 1999; Gopurenko and Hughes, 2002; Wee et al., 2015), and has been attributed to the role of Sundaland as a land barrier during past glaciation periods (Wee et al., 2015).

Within the Pacific or Indian Ocean populations, no genetic differentiation or distinct lineages between populations were identified. A homogeneous phylogeographic pattern was seen in the Chinese populations, and the same result was found in Pakistan. Meanwhile, similar results were found in this species along the coast of China using mitochondrial Cytb and COI gene sequences (Sun and Tang, 2018; Sun et al., 2018). In general, ocean currents play an important role in transporting the larvae of marine organisms (Liu et al., 2007). *P. chinensis* is speculated to travel over a long range, considering its larval stage and the velocity of currents near the Chinese and Pakistani coasts. Therefore, larvae and juveniles from the coastal spawning of one population could travel on certain currents, and the connectivity may be high among populations within one geographic group (Liu et al., 2007, 2012). This possibility may offer sufficient evidence for explaining the low level of genetic divergence of *P. chinensis* within groups in China or Pakistan (Sun et al., 2013).

4.3 Historical demography

Given the neutrality tests resulting in a high h value and a low π value, *P. chinensis* populations along the Indo-Pacific Ocean may have experienced a population expansion. During Pleistocene glaciations, sea levels fluctuated repeatedly, dropping as low as 200 m below present levels and occasionally rising above, present levels, thereby changing the seaways between the Indian and Pacific Oceans (Galloway and Kemp, 1981). Those changes would have had a profound influence on the distributions, abundances, and demographic dynamics of *P. chinensis*. Throughout much of the Pleistocene, the Strait of Malacca was closed, and the gene flow between the Pacific and Indian Oceans may have been restricted. Thus, dispersal was unlikely to have occurred either in the past or at present. As with other marine fauna (Gopurenko and Hughes, 2002; Liu et al., 2007; Wee et al., 2015), *P. chinensis* was likely to have contracted into geographically isolated places of refuge during glacial advances, with massive extinction and a significant reduction in population size and to have expanded during interglacial periods to quickly recolonize previously glaciated coastal areas and newly available habitats. In response to these changes, most temperate taxa were forced into repeated cycles of refugial retreat during glacial periods and expansion during interglacial periods.

The previous scenario offers a plausible explanation that the Malay Peninsula acted as a border between the two biogeographic regions to prevent or restrict the dispersal of many marine species between the Indian and Pacific Oceans for thousands of years (Raynal et al., 2014; Yellapu et al., 2016). Afterward, *P. chinensis* adapted to a different spectrum of salinity, temperature, and habitats and facilitated a different population structure.

Unfortunately, we collected only four geographical populations of *P. chinensis*, which do not sufficiently represent its entire distribution. The results of population genetics of this species in this study may be one-sided; thus, further studies are needed, including those collecting *P. chinensis* samples with an intermediate distribution, to confirm our results.

4.4 Conclusions and implications for conservation and management

The genetic population diversity and the genetic structure of marine fish must be assessed for fishery management and conservation. The contemporary genetic structure of *P. chinensis* revealed in this study can improve genetic knowledge and provide a firm basis for defining spatial boundaries of fishery stocks in the Indo-Pacific Oceans. In the future, science-based management should implement distinct regions of fishery management for this species.

The current study also provides different insights into genetic heterogeneity occurring within other similar distributed species instead of within a single panmictic population. The presence of a spatial subdivision identified here should encourage future research to investigate (1) other possible assemblages/clades that may exist, especially along the coastal waters in Southeast Asia, (2) whether a distribution exists in the Strait of Malacca, and (3) the influence of fishing pressure on *P. chinensis* stocks in distinct fishery regions (Williams et al., 2015). Therefore, all objectives need to be addressed by expanding the sampling effort to incorporate more locations (e.g., the Gulf of Oman, the Arabian Sea, the Bay of Bengal, and the Andaman Sea) and temporal samples.

Acknowledgments. The present study could not have been performed without assistance from Dr. Fozia Khan Siyal and Prof. Sun Dianrong in specimen collection of *Pampus chinensis*. The authors declare no conflict of interest. This research was supported by the National Natural Science Foundation of China (41776171), the National Programme on Global Change and Air-Sea Interaction (GASI-02-PAC-YDspr/sum/aut and GASI-02-SCS-YSWspr/aut), the National Key Research and Development Program of China (2018YFC1406302), the Scientific Startup Foundation of Zhejiang Ocean University (Q1505), and the Scientific Research Foundation of Third Institute of Oceanography, SOA (2016010).

References

- Avice JC. 2009. Phylogeography: retrospect and prospect. *J Biogeogr* 36: 3–15.
- Barnes TC, Junge C, Myers SA, Taylor MD, Rogers PJ, Ferguson GJ, Lieschke JA, Donnellan SC, Gillanders BM. 2015. Population structure in a wide-ranging coastal teleost (*Argyrosomus japonicus*, Sciaenidae) reflects marine biogeography across southern Australia. *Mar Freshw Res* 67: 1103–1113.
- Benzie JAH. 1999. Major genetic differences between crown-of-thorns starfish (*Acanthaster planci*) populations in the Indian and Pacific Oceans. *Evolution* 53: 1782–1795.
- Benzie JAH, Ballment E, Forbes AT, Demetriades NT, Sugama Haryanti K, Moria S. 2002. Mitochondrial DNA variation in Indo-Pacific populations of the giant tiger prawn, *Penaeus monodon*. *Mol Ecol* 11: 2553–2569.
- Bermingham ES, McCaVerty A, Martin P. 1997. Fish biogeography and molecular clocks: perspectives from the Panamanian Isthmus, in: T. Kocher, C. Stepien (Eds.), *Molecular Systematics of Fishes*, Academic Press, San Diego, pp. 113–126.
- Bowen BW, Bass AL, Rocha LA, Grant WS, Robertson DR. 2001. Phylogeography of the trumpet fishes (*Aulostomus*): ring species complex on a global scale. *Evolution* 55: 1029–1039.
- Chenoweth SF, Hughes JM, Keenan CP, Lavery S. 1998. When oceans meet: a teleost shows secondary intergradation at an Indian-Pacific interface. *Proc R Soc Lond B Biol Sci* 265: 415–420.
- Divya PR, Vineesh N, Ayyathurai K, Basheer VS, Achamveetil G. 2018. Population structure of Spanish mackerel *Scomberomorus commerson* (Lacepède, 1800) in the Northern Indian Ocean determined using microsatellite markers. *Aquat Living Resour* 31: 22. DOI: [10.1051/alr/2018011](https://doi.org/10.1051/alr/2018011).
- Drummond AJ, Suchard MA, Xie D, Rambaut A. 2012. Bayesian phylogenetics with BEAUti and the BEAST 1.7. *Mol Biol Evol* 29: 1969–1973.
- Excoffier L, Laval G, Schneider S. 2005. Arlequin (version 3.0): an integrated software package for population genetics data analysis. *Evol Bioinform* 1: 47–50.
- Galloway RW, Kemp EM. 1981. Late Cainozoic environments in Australia, in: A. Keast (Ed.), *Ecological Biogeography of Australia*, Dr. W. Junk Publishers, Hague, 51–80.
- Giles JL, Ovenden JR, Almojil D, Garvilles E, Khampetch KO, Manjebraayakath H, Riginos C. 2014. Extensive genetic population structure in the Indo-West Pacific spot-tail shark, *Carcharhinus sorrah*. *Bull Mar Sci* 90: 427–454.
- Gopurenko D, Hughes JM. 2002. Regional patterns of genetic structure among Australian populations of the mud crab, *Scylla serrata* (Crustacea: Decapoda): evidence from mitochondrial DNA. *Mar Freshw Res* 53: 849–857.
- Goude J. 2001. FSTAT, Version 2.9.3: a program to estimate and test gene diversities and fixation indices.
- Koizumi I, Yamamoto S, Maekawa K. 2006. Decomposed pairwise regression analysis of genetic and geographic distances reveals a metapopulation structure of stream-dwelling Dolly Varden charr. *Mol Ecol* 15: 3175–3189.
- Latch EK, Dharmarajan G, Glaubitz JC, Rhodes OE, Jr. 2006. Relative performance of Bayesian clustering software for inferring population substructure and individual assignment at low levels of population differentiation. *Conserv Genet* 7: 295–302.
- Lavery S, Moritz C, Fielder DR. 1996. Indo-Pacific population structure and evolutionary history of the coconut crab *Birgus latro*. *Mol Ecol* 5: 557–570.
- Liu J, Li C, Li X. 2002. Studies on Chinese pomfret fishes of the genus *Pampus* (Pisces: Stromateidae). *Studia Marina Sinica* 44: 240–252.
- Liu J, Gao T, Wu S, Zhang Y. 2007. Pleistocene isolation in the Northwestern Pacific marginal seas and limited dispersal in a marine fish, *Chelon haematocheilus* (Temminck & Schlegel, 1845). *Mol Ecol* 16: 275–288.
- Liu M, Lin L, Gao T, Yanagimoto T, Sakurai Y, Grant WS. 2012. What maintains the central North Pacific genetic discontinuity in Pacific herring? *PLoS One* 7: e50340. DOI: [10.1371/journal.pone.0050340](https://doi.org/10.1371/journal.pone.0050340).

- Lu P, Yorkson M, Morden CW. 2016. Population genetics of the endemic Hawaiian species *Chrysodracon hawaiiensis* and *Chrysodracon auwahiensis* (Asparagaceae): insights from RAPD and ISSR variation. *Int J Mol Sci* 17: 1341. DOI: [10.3390/ijms17081341](https://doi.org/10.3390/ijms17081341).
- Luikart G, Cornuet JM. 1998. Empirical evaluation of a test for identifying recently bottlenecked populations from allele frequency data. *Conserv Biol* 12: 228–237.
- Ovenden JR. 2013. Crinkles in connectivity: combining genetics and other types of biological data to estimate movement and interbreeding between populations. *Mar Freshw Res* 64: 201–207.
- Pillai VN, Menon NG. 2000. Marine fisheries research and management, Central Marine Fisheries Research Institute, Kochi, India, pp. 364–373.
- Piry S, Luikart G, Cornuet JM. 1999. BOTTLENECK: a computer program for detecting recent reductions in the effective population size using allele frequency data. *J Hered* 90: 502–503.
- Pritchard JK, Stephens M, Rosenberg NA, Donnelly P. 2000. Association mapping in structured populations. *Am J Hum Gene* 67: 170–181.
- Qiu F, Li H, Lin H, Ding S, Miyamoto MM. 2016. Phylogeography of the inshore fish, *Bostrychus sinensis*, along the Pacific coastline of China. *Mol Phylogenet Evol* 96: 112–117.
- Raymond M, Rousset F. 1995. GENEPOP (version 1.2): population genetics software for exact tests and ecumenicism. *J Hered* 86: 248–249.
- Raynal JM, Crandall ED, Barber PH, Mahardika GN, Lagman MC, Carpenter KE. 2014. Basin isolation and oceanographic features influencing lineage divergence in the humbug damselfish (*Dascyllus aruanus*) in the Coral Triangle. *B Mar Sci* 90: 513–532.
- Sambrook J, Fritsch EF, Maniatis T. 1989. Molecular cloning. Cold Spring Harbor Laboratory Press, New York.
- Selkoe KA, Toonen RJ. 2011. Marine connectivity: a new look at pelagic larval duration and genetic metrics of dispersal. *Mar Ecol Prog Ser* 436: 291–305.
- Siyal FK. 2013. Some aspects of biology, in: Molecular Phylogeography and Maximum Sustainable Yield Estimates of Genus *Pampus* (Family Stromateidae), Ocean University of China, Qingdao.
- Slatkin M. 1987. Gene flow and the geographic structure of natural populations. *Science* 236: 787–792.
- Sukumaran S, Sebastian W, Gopalakrishnan A. 2017. Genetic population structure and historic demography of Indian mackerel, *Rastrelliger kanagurta* from Indian peninsular waters. *Fish Res* 191: 1–9.
- Sun P, Tang BJ. 2018. Low mtDNA variation and shallow population structure of the Chinese pomfret *Pampus chinensis* along the China coast. *J Fish Biol* 92: 214–228.
- Sun P, Tang BJ, Yin F. 2018. Population genetic structure and genetic diversity of Chinese pomfret at the coast of the East China Sea and the South China Sea. *Mitochondrial DNA A* 29: 643–649.
- Sun P, Yin F, Gao Q, Shi Z. 2013. Genetic diversity and population structure of silver pomfret (*Pampus argenteus*) in the Indo–West Pacific revealed by mitochondrial control region sequences. *Biochem Syst Ecol* 51: 28–36.
- Sun P, Tang BJ, Yin F. 2017. Population genetic structure and genetic diversity of Chinese pomfret at the coast of the East China Sea and the South China Sea. *Mitochondrial DNA A* 29: 643–649. DOI: [10.1080/24701394.2017.1334773](https://doi.org/10.1080/24701394.2017.1334773).
- Tamura K, Peterson D, Peterson N, Stecher G, Nei M, Kumar S. 2011. MEGA5: molecular evolutionary genetics analysis using maximum likelihood, evolutionary distance, and maximum parsimony methods. *Mol Biol Evol* 28: 2731–2739.
- Van Oosterhout C, Hutehinson WF, Wills DPM, Shipley P. 2004. Micro-checker: software for identifying and correcting genotyping errors in microsatellite data. *Mol Ecol Notes* 4: 535–538.
- Wang P, Sun X. 1994. Last glacial maximum in China: comparison between land and sea. *Catena* 23: 341–353.
- Wee AKS, Takayama K, Chua JL, Asakawa T, Meenakshisundaram SH, Onrizal Adjie B, Ardli ER, et al. 2015. Genetic differentiation and phylogeography of partially sympatric species complex *Rhizophora mucronata* Lam. and *R. stylosa* Griff. using SSR markers. *BMC Evol Biol* 15: 1–13.
- Williams ST, Benzie JAH. 1998. Evidence of a biogeographic break between populations of a high dispersal starfish: congruent regions within the Indo–West Pacific defined by color morphs, mtDNA, and allozyme data. *Evolution* 52: 87–99.
- Williams SM, Bennett MB, Pepperell JG, Morgan JAT, Ovenden JR. 2015. Spatial genetic subdivision among populations of the highly migratory black marlin *Istiompax indica* within the central Indo-Pacific. *Mar Freshw Res* 67: 1205–1214.
- Yamada U, Tokimura M, Hoshino K, Deng S, Zheng Y, Li S, Kim Y, Kim J. 2009. Name and illustrations of fish from the East China Sea and the Yellow Sea: Japanese, Chinese, Korean, Overseas Fishery Cooperation Foundation of Japan, Tokyo, pp. 525–528.
- Yang W, Li J, Yue G. 2006. Multiplex genotyping of novel microsatellites from silver pomfret (*Pampus argenteus*) and cross-amplification in other pomfret species. *Mol Ecol Notes* 6: 1073–1075.
- Yeh FC, Yang R, Boyle TJ, Ye Z, Xiyan JM. 2000. PopGene32, Microsoft Windows-based freeware for stock genetic analysis, version 1.32, Molecular Biology and Biotechnology Centre, University of Alberta, Edmonton, Alberta, Canada.
- Yellapu B, Jeffs A, Battaglene S, Lavery DS. 2016. Population subdivision in the tropical spiny lobster *Panulirus ornatus* throughout its Indo–West Pacific distribution. *ICES J Mar Sci* 74: 759–768.
- Zeng L, Cheng Q, Chen X. 2012. Microsatellite analysis reveals the population structure and migration patterns of *Scomber japonicus* (Scombridae) with continuous distribution in the East and South China Seas. *Biochem Syst Ecol* 42: 83–93.
- Zheng Y, Chen X, Cheng J, Wang Y, Shen X, Chen W. 2003. Biological resources and environment of the continental shelf of East China Sea. Shanghai Science and Technology Press, Shanghai, pp. 379–388.

Cite this article as: Li Y, Gao T, Zhou Y, Lin L. 2019. Spatial genetic subdivision among populations of *Pampus chinensis* between China and Pakistan: testing the barrier effect of the Malay Peninsula. *Aquat. Living Resour.* 32: 8